Parametric Study of Long-term Deflections of Reinforced Recycled Aggregate Concrete Members According to the fib Model Code 2010

NikolaTošić*,a, Albert de la Fuenteb, Snežana Marinkovićc

a Assistant prof. Dr. Department for Materials and Structures. Faculty of Civil Engineering. University of Belgrade. Bulevar kralja Aleksandra 73, 11000 Belgrade, Serbia. ntosic@imk.grf.bg.ac.rs

b Associate prof. Dr. Civil and Environmental Engineering Department. Universitat Politécnica de Catalunya. Jordi Girona 1–3, 08034 Barcelona, Spain. albert.de.la.fuente@upc.edu

c Prof. Dr. Department for Materials and Structures. Faculty of Civil Engineering. University of Belgrade. Bulevar kralja Aleksandra 73, 11000 Belgrade, Serbia. sneska@imk.grf.bg.ac.rs

ABSTRACT

In this study, a parametric analysis of the deflection calculations of reinforced RAC members is presented. Within the parametric analysis, member support conditions, ambient conditions (influencing shrinkage and creep), reinforcement ratios, and quasi-permanent–to–design load ratios are varied. Through the analysis, the change in deflections is observed against RCA percentage (from NAC to RAC with 100% of coarse RCA) and span-to-effective depth ratio. The results of the analysis enable a clear overview of the variability of the deflections of RAC members relative to NAC.

KEYWORDS: recycled aggregate concrete, beam, shrinkage, creep, deflection, Model Code 2010.

1. Introduction

Serviceability limit states (SLS), and more specifically, deflection control is becoming an increasingly important aspect of structural design although traditionally, more attention has been paid to ultimate limit states (ULS). However, deflection control is still among the most complex aspects of reinforced concrete (RC) design, mostly because of the large number of influencing factors such as the geometrical properties of the member, moduli of elasticity of concrete and reinforcement, concrete tensile strength, area and distribution of reinforcement, load intensity and history, stiffness reduction caused by cracking and tension stiffening, member structural system, and moment redistribution in statically indeterminate systems [1]. Furthermore, the relatively good precision of mathematical models for other aspects of reinforced concrete behaviour has unreasonably led many engineers to trust SLS models too much when in fact they are often associated with a large uncertainty even when predicting experimental results obtained under controlled conditions [2]. Hence, deflection control should be thought of more as providing a "measure of deformability" of an RC member then a precise prediction of deflections.

Among existing deflection control models, documents such as the *fib* Model Code

2010 [3] provide several methods ranging from general methods of curvature integration to indirect span-to-effective depth limits. However, these methods have been developed several decades ago and calibrated on traditional RC members [4]. In recent years, a range of new concrete types has been emerging, with a significant number focused on incorporating recycled and waste materials into concrete. Such "green" concretes are motivated by the fact that concrete production causes a significant impact on the environment: global annual production of cement is responsible for 7–10% of all anthropogenic CO_2 emissions [5] and almost 50% of all waste generated is construction and demolition waste (of which half is concrete waste) [6].

One of the most studied types of green concrete has been recycled aggregate concrete (RAC), produced with crushed concrete waste in the form of recycled concrete aggregate (RCA). RAC has been comprehensively studied on both material and structural levels [7–10]. The considerable knowledge obtained on RAC has finally reached a stage at which structural design of RAC can be incorporated into new design codes. In this context, ULS design of RAC was shown to be possible using existing design provisions for natural aggregate concrete (NAC). However, experimental results have shown large differences in the modulus of elasticity, shrinkage and creep between RAC and "companion NAC" (produced with identical effective water-cement ratios) – largely a consequence of the residual mortar attached to RCA [8,11,12]. In turn, this also leads to larger deflections of RAC members and the need to modify deflection control models [13]. Hence, a thorough analysis of the implications of different RAC deflection control needs to be taken into account.

The aim of this study is to present a parametric study of long-term deflections of reinforced RAC members calculated using the *fib* Model Code 2010 and already proposed corrections for RAC. For the purpose of this study, RAC will refer to concrete in which only the coarse aggregate fraction (particle size > 4 mm) is replaced by RCA.

First, a brief overview of RAC deflection control is given in Section 2. Then, the parametric study and its results are presented in Section 3. The deformability of RAC and companion NAC is compared for different values of influencing parameters such as span-effective depth ratios, service load-to-design load rations, shrinkage strains, and creep coefficients. Finally, conclusions of the study are presented in Section 4.

2. Deflections of RAC members

2.1 Deflection control in fib Model Code 2010

The most general method of deflection control in the *fib* Model Code 2010 is the integration of curvatures. For RC members loaded above the cracking load, this general method consists of a sectional analysis based on the interpolation of curvatures between two distinct states [3]: state 1, the uncracked state in which the full area of the concrete cross-section is effective, and state 2, the fully-cracked state in which cracked concrete is ignored, i.e., the cross-section is composed of reinforcement in tension and concrete in compression. A simplified approach is also possible, in which curvatures are not interpolated, but directly deflections, calculated separately for states 1 and 2.

The interpolation between states 1 and 2 is performed using a distribution coefficient ζ (hence the method is sometimes called the ζ-method). For pure bending, ζ is defined as

$$\zeta = \begin{cases} 1 - \beta \cdot \left(\dfrac{M_{cr}}{M_{max}}\right)^2 & ; \ M_{max} \geq \sqrt{\beta} \cdot M_{cr} \\ 0 & ; \ M_{max} < \sqrt{\beta} \cdot M_{cr} \end{cases} \quad (1)$$

where β is a coefficient taking into account load duration:

$$\begin{aligned} \beta = 1.0 \quad & \text{single, short} - \text{term loading} \\ \beta = 0.5 \quad & \text{sustained, repeated loading} \end{aligned} \quad (2)$$

M_{cr} is the cracking moment and M_{max} is the maximum moment in the span of the member (or end of a cantilever), usually taken as the

maximum value that is expected in service (e.g., from the characteristic load combination).

Using the ζ coefficient, deflections are interpolated as follows:

$$a = \zeta \cdot a_2 + (1 - \zeta) \cdot a_1 \qquad (3)$$

where a is the final deflections, whereas a_1 and a_2 are deflections in states 1 and 2, respectively. The deflections in states 1 and 2 are composed of a component due to load a_{load} and a component due to shrinkage a_{cs} and are calculated as

$$a_{load,n} = K \cdot \frac{M_{max} \cdot l^2}{E_{c,ef} \cdot I_{i,n}} \qquad (4)$$

$$a_{cs,n} = \delta_{cs} \cdot \varepsilon_{cs}(t, t_s) \cdot \frac{S_{i,n} \cdot l^2}{I_{i,n} \cdot 8} \qquad (5)$$

where n can take values 1 or 2; K depends on the statical system (e.g., 0.104 for a simply supported beam under uniformly distributed load); $I_{i,n}$ is the moment of inertia of the transformed section; $S_{i,n}$ is the first moment of area of the reinforcement about the transformed section's centroid; $\varepsilon_{cs}(t, t_s)$ is the concrete shrinkage strain at time t with drying initiation at time t_s; δ_{cs} depends on the statical system (e.g., 1 for a simply supported beam); and the effect of creep is taken into account using the effective modulus of elasticity $E_{c,ef}$:

$$E_{c,ef} = \frac{E_{cm}}{1 + \varphi(t, t_0)} \qquad (6)$$

In Eq. (6), $\varphi(t, t_0)$ is the creep coefficient of concrete loaded at time t_0, at time t, and E_{cm} is the modulus of elasticity of concrete at 28 days.

2.2 Deflection control corrections for RAC

Typically, in SLS design, values of input parameters are calculated based on concrete class and exposure conditions. For deflection control and the *fib* Model Code 2010 that means that the values of the modulus of elasticity, tensile strength, shrinkage strain and creep coefficient are calculated based on concrete compressive strength and parameters such as member dimensions, relative humidity and temperature [3].

So far, researchers have done significant work on determining whether existing code provisions are valid for the case of RAC. For tensile strength, Silva et al. [14] demonstrated that the Eurocode 2 equation (equivalent to the Model Code 2010 expression) based on mean compressive strength is applicable to RAC.

For the modulus of elasticity, Silva et al. [11] showed that a significant reduction exists between RAC and companion NAC. The *fib* Model Code 2010 expression for modulus of elasticity is

$$E_{cm} = 21500 \cdot \alpha_E \cdot \left(\frac{f_{cm}}{10}\right)^{1/3} \qquad (7)$$

where a_E is a coefficient dependent on the type of natural aggregate (e.g., 1.0 for quartzite aggregates) and f_{cm} is the mean compressive strength of concrete. Based on the findings of Silva et al. [14], Tošić et al. [13] proposed the following correction for the a_E coefficient:

$$\alpha_E = 1.0 - 0.3 \cdot \frac{RCA\%}{100} \qquad (8)$$

The correction leads to a maximum reduction of E_{cm} of 30% in the case of RAC produced with 100% of coarse RCA (RAC100) relative to NAC. For shrinkage and creep Tošić et al. [8,12] proposed global correction factors to be applied to shrinkage strain and creep coefficient calculated using Model Code 2010:

$$\varepsilon_{cs,RAC}(t, t_s) = \xi_{cs,RAC} \cdot \varepsilon_{cs}(t, t_s) \qquad (9)$$
$$\varphi_{RAC}(t, t_0) = \xi_{cc,RAC} \cdot \varphi(t, t_0) \qquad (10)$$

The shrinkage and creep correction factors ξ_{cs} and ξ_{cc}, respectively, depend on RAC compressive strength and RCA percentage:

$$\xi_{cs,RAC} = \left(\frac{RCA\%}{f_{cm}}\right)^{0.30} \geq 1.0 \qquad (11)$$

$$\xi_{cc,RAC} = 1.12 \cdot \left(\frac{RCA\%}{f_{cm}}\right)^{0.15} \geq 1.0 \qquad (12)$$

Finally, Tošić et al. [13] proposed changes to the interpolation coefficient ζ, i.e., the empirical coefficient β in Eq. (1):

$$\begin{array}{l} \beta_{RAC} = 0.75 \ \text{single, short} - \text{term loading} \\ \beta_{RAC} = 0.25 \ \text{sustained, repeated loading} \end{array} \qquad (13)$$

Hence, using all the corrections presented in Eqs. (8)–(13), deflection control of RAC, equal in performance to deflection control of NAC, is possible [13].

3. Parametric study on RAC deflections

Since a complete procedure for deflection control of RAC is available, an investigation should be carried out into the implications on structural design. Therefore, a parametric study is performed in this study to quantify the differences in deflection behavior between RAC and NAC considering the proposed modifications of the *fib* Model Code 2010.

3.1 Deformability of RAC relative to NAC

The first analysis in this study is on the differences in RAC and NAC deformability, i.e., how much larger are RAC deflections compared with NAC considering equal loading, geometry, and boundary conditions.

For this purpose, a simply supported one-way slab is considered (considering a 1-m wide strip, i.e., $b = 1000$ mm). The height h and effective depth d of the slab are taken as 230 and 200 mm, respectively. The ULS design load q_{Ed} of the slab is taken as 15 kN/m². Concrete class is C30/37 ($f_{cm} = 38$ MPa). Three concretes are considered: NAC, RAC50, and RAC100 with 0%, 50%, and 100% of coarse RCA.

The span of the slab L is varied by adopting L/d ratios from 10 to 40 (i.e., from 2000 to 8000 mm, in steps of 400 mm). For each span, ULS-required tensile reinforcement $A_{s,ULS}$ is calculated, controlling for minimum reinforcement (0.013%). Then, deflections are calculated using the simplified ζ-method of interpolating deflections, using the following parameters. The quasi-permanent load q_{qp} is varied as 50%, 60%, and 70% of the design load q_{Ed}, but the maximum bending moment in Eq. (1) is calculated using the characteristic load taken as $q_{rare} = 1.25 \cdot q_{qp}$ (to take into account possibly larger cracking during the service life of a member). The loading age is taken as 28 days.

Tensile strength f_{ctm} (necessary for calculating M_{cr}) is calculated from f_{cm} according to Model Code 2010, identically for NAC, RAC50, and RAC100. The modulus of elasticity E_{cm} is calculated using Eqs. (7) and (8). Initially, for NAC, the shrinkage strain ε_{cs} and creep coefficient φ are taken as 0.4‰ and 2.2, respectively. Then, Eqs. (11) and (12) are applied for RAC50 and RAC100. Deflections are therefore calculated for three levels of quasi-permanent load, for three concretes NAC, RAC50, and RAC100 (with equal tensile reinforcements and M_{cr}, but different E_{cm}, ε_{cs}, and φ). Deflections a calculated for each L/d ratio are divided by the deflection limit a_{lim} for the corresponding L/d ratio, with $a_{lim} = L/250$ [3]. The obtained result is shown in Figure 1.

Several conclusions follow from Figure 1. First, as expected, for low L/d ratios, deflections are very small; minimum reinforcement is ruling up until $L/d = 18$. Once reinforcement becomes larger than $A_{s,min}$, deflection start increasing rapidly and the a/a_{lim} ratio quickly becomes larger than 1. It can be clearly seen that the a/a_{lim} ratio is larger for RAC than NAC, but the relative differences remain independent of load level, e.g., at $L/d = 40$, the ratio of a/a_{lim} between RAC50 and NAC is 1.10 and RAC100 and NAC 1.25 for all load levels.

As expected for a one-way slab with $d = 200$ mm and a load typical for residential buildings, the deflection limit is reached between $L/d = 20$ and 25, depending on the load level. For $q_{qp} = 0.5 \cdot q_{Ed}$, limit deflections are reached for $L/d = 26$, 25, and 24 for NAC, RAC50, and RAC100, respectively; for $q_{qp} = 0.6 \cdot q_{Ed}$, limit deflections are reached for $L/d = 23$, 22, and 21 for NAC, RAC50, and RAC100, respectively; and for $q_{qp} = 0.7 \cdot q_{Ed}$, limit deflections are reached for $L/d = 21$, 20.5, and 20 for NAC, RAC50, and RAC100, respectively. In other words, NAC members could have 200–400 mm longer spans compared with RAC100 for precisely satisfied deflections; though differences become larger as L/d increases.
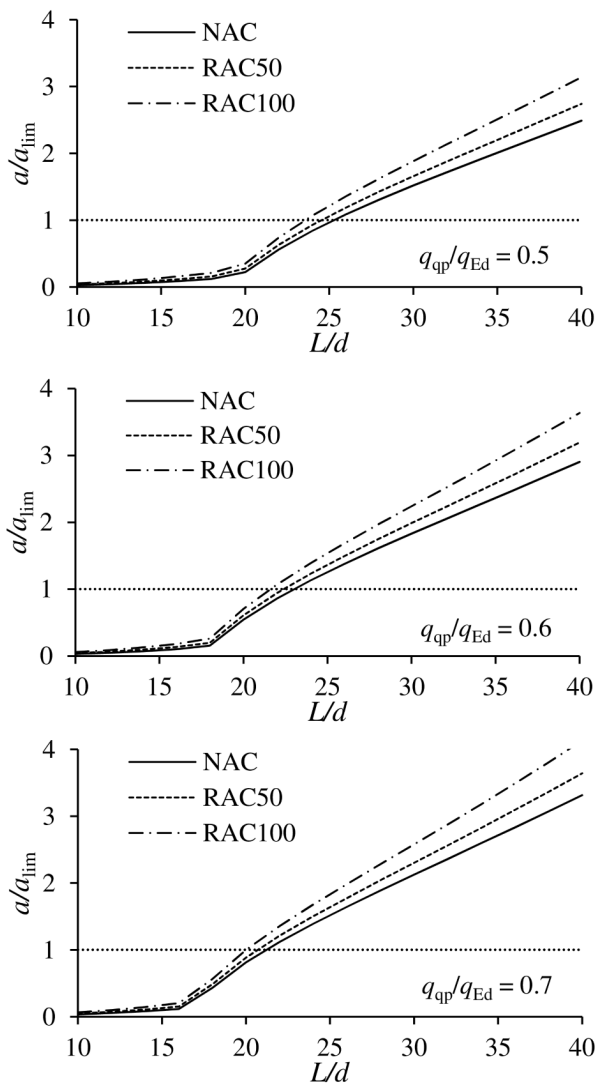
Figure 1. Normalized deflections vs. L/d ratio for NAC, RAC50, and RAC100 and different load levels.

Of course, the obtained results are only valid for the selected set of parameters. Among the most important influencing factors on deflections are shrinkage and creep. Therefore, in order to test the sensitivity of the conclusions to shrinkage and creep, their values were varied. The analysis was performed for NAC and RAC100 and for $q_{qp} = 0.6 \cdot q_{Ed}$ by calculating new a/a_{lim} vs. L/d were calculated using two sets of ε_{cs} and φ: 0.3‰ and 2.0 as a lower bound, and 0.5‰ and 2.4 as an upper bound. Both sets were adopted for NAC and increased for RAC100 using Eqs. (11) and (12).

The results are shown in Figure 2. It is clearly seen that the two shaded areas do not overlap at all. Hence, RAC100 deflections are significantly different and larger than NAC, or, in other words, RAC100 members are significantly more deformable compared with NAC members.

3.2 Increase of RAC member depth relative to NAC

In the previous section, it was shown that for identical geometric properties and reinforcement, RAC deflections are larger than NAC deflections. However, in design, engineers will have to satisfy deflections. Therefore, changes in design must be made to RAC members in order to satisfy deflection limits. One approach is to increase the depth/height of RAC members. It is very important to determine how much deeper/higher should RAC members be relative to NAC to satisfy deflections ($a_{lim} = L/250$), as this will have significant economic impact and influence the willingness of engineers to use RAC.

For this purpose, the following analysis was performed. Again, a simply supported one-way slab is considered. For NAC, as before, $h = 230$ mm and $d = 200$ mm is adopted with L/d varying between 10 and 40. In this section, only $q_{qp} = 0.6 \cdot q_{Ed}$ is considered with ε_{cs} and φ equal to 0.4‰ and 2.0 for NAC, respectively; Eqs. (11) and (12) are used for RAC50 and RAC100. However, in this case, for each L/d ratio, the design load q_{Ed} (and $A_{s,ULS}$) was determined so that $a = a_{lim}$. In other words, q_{Ed} is not constant (as in the previous section), but $a = a_{lim}$ for each L/d ratio.

Because of smaller E_{cm} and larger ε_{cs}, and φ, RAC50 and RAC100 cannot satisfy $a = a_{lim}$. Hence, their depth must be increased. In this analysis, the tensile reinforcement center of gravity was always taken 30 mm from the bottom surface. Then, the effective depth d_{RAC} of RAC50 and RAC100 was increased (rounded up to 5 mm) for each L/d ratio (and height was determined as $h = d_{RAC} + 30$ mm). In this way, for each L/d value, a ratio of RAC-to-NAC effective depths, d_{RAC}/d_{NAC}, could be determined.
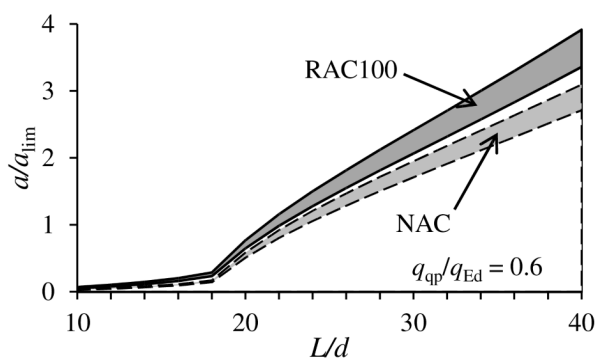
Figure 2. NAC and RAC100 normalized deflections vs. L/d ratio for upper and lower bound values of shrinkage strain and creep coefficient.

Figure 3. Ratio of RAC-to-NAC effective depth for varying L/d ratios

The results are shown in Figure 3. The d_{RAC}/d_{NAC} ratio decreases with increasing L/d. For $L/d = 10$, the values are 1.08 and 1.18 for RAC50 and RAC100, respectively, i.e., effective depths are 215 and 235 mm, respectively, compared with 200 mm for NAC. Heights are 245 and 265 mm, respectively, compared with 230 mm for NAC.

However, the d_{RAC}/d_{NAC} quickly decreases and ends at 1.03 and 1.05 for RAC50 and RAC100, respectively, at $L/d = 40$ (effective depth differences are 5 and 10 mm, respectively). In the range of typical L/d ratios for these members (20–30), d_{RAC}/d_{NAC} is from 1.05 to 1.03 for RAC50 and 1.10 to 1.08 for RAC100 (decreasing with increasing L/d).

These results are encouraging for the use of RAC as the differences in effective depth do not exceed 10%. Of course, the results are valid only for the range of parameters selected in this study. An additional encouragement toward using RAC is that, for differences of this magnitude, the problem of deflections can be satisfied in other ways, besides increasing member depth.

3.3 Increase of RAC member reinforcement relative to NAC

In the previous section it was shown that in the typical L/d range for one-way slabs, the effective depth of RAC members needn't be more than 10% higher than that of NAC members in order to satisfy deflection criteria.
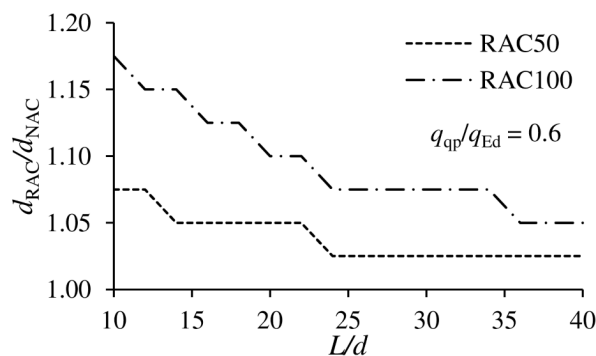
In this section, an alternative to increasing member effective depth/height will be investigated – increasing tensile reinforcement.

Parameters identical to section 3.1 are adopted, but only $q_{qp} = 0.6 \cdot q_{Ed}$ is considered and the 'critical' range of $L/d = 20$–25 is analyzed. Now, instead of maintaining tensile reinforcement as required from ULS design ($A_{s,ULS}$), it is increased as much as necessary in order to obtain $a \leq a_{lim}$. As stated in section 3.1, for $q_{qp} = 0.6 \cdot q_{Ed}$, deflections are larger than the limit only for L/d greater than 23, 22, and 21 for NAC, RAC50, and RAC100, respectively. Therefore, these cases do not require an increase in tensile reinforcement above $A_{s,ULS}$. Above these L/d ratios, the necessary additional tensile reinforcement incrases rapidly. The results are shown in Table 1.

Table 1. Necessary tensile reinforcement increase in order to achieve $a \leq a_{lim}$ for $L/d = 20$–25

L/d	$A_s/A_{s,ULS}$		
	NAC	RAC50	RAC100
20	1.00	1.00	1.00
21	1.00	1.00	1.00
22	1.00	1.00	**1.16**
23	1.00	**1.19**	**1.67**
24	**1.26**	**1.55**	**2.42**
25	**1.56**	**2.00**	**3.57**

A meaningful increase in tensile reinforcement for the purpose of satisfying deflection control could be considered up to 100% (i.e., $A_s/A_{s,ULS} = 2.0$), and this only over a short length in the zone of maximum bending. Then, Table 1 demonstrates that for NAC the L/d ratio can be extended up to 25 (an increase

in span of 400 mm). For RAC50, this increase is also up to $L/d = 25$, whereas for RAC100 it is only up to $L/d = 23$. In other words, by only increasing tensile reinforcement, RAC50 slabs can be comparable to NAC. Further considering that optimal replacement ratios—in terms of environmental and economic impact—is precisely RAC50 [15], this result is very positive for the use of RAC. Finally, even though RAC100 remains somewhat inferior to NAC in terms of service behavior, the differences are not significant to prevent its successful use in structural applications.

4. Conclusions

This study presented the results of a parametric investigation into the long-term deflections of reinforced RAC one-way slabs, in relation to NAC. Different analyses and approaches were undertaken in order to determine the differences in deformability between RAC and NAC members. The simplified ζ-method of the *fib* Model Code 2010 was used with corrections for RAC, concerning the modulus of elasticity, shrinkage strain, creep coefficient, and interpolation coefficient ζ [8,12,13]. For the values of parameter ranges adopted in this study, the following conclusions are drawn:

- RAC50 and RAC100 deflections are larger than NAC deflections over the entire considered L/d range, independent of load level and without strong sensitivity to shrinkage and creep;
- The ratio of normalized deflections a/a_{lim} between RAC50 or RAC100 and NAC remains almost constant over the considered L/d range;
- Depending on the load level, deflections are satisfied up to $L/d = 21$–26 for NAC, 20.5–25 for RAC50, and 20–24 for RAC100;
- In order to precisely satisfy deflections with $a = a_{\mathrm{lim}}$, greater effective depths of RAC members are necessary compared with NAC. The increase in RAC member depth

decreases with increasing L/d ratio, $d_{\mathrm{RAC}}/d_{\mathrm{NAC}}$ goes from 1.18 to 1.05 for RAC100 and from 1.08 to 1.03 for RAC50, from $L/d = 10$ to 40;

- If an increase in tensile reinforcement is used to satisfy deflections and is limited to 100%, the range of satisfied deflections can be extended from 23 to 25 for NAC, 22 to 25 for RAC50 and 21 to 23 for RAC100.

Although this study considers only a small range of parameter values, its results are a positive sign for the practical implementation of RAC in reinforced structures. Further analyses considering different boundary conditions, geometries, ambient conditions, as well as construction sequences should be performed to further verify the results of this study.

References

[1]   N. Pecić, Improved method for deflection control of reinforced concrete structures, Faculty of Civil Engineering, Belgrade University, 2012.

[2]   A.W. Beeby, S. Narayanan, Designer's guide to Eurocode 2: Design of concrete structures, Thomas Telford, London, 2005.

[3]   FIB, fib Model Code for Concrete Structures 2010, International Federation for Structural Concrete (fib), Lausanne, 2013. doi:10.1002/9783433604090.

[4]   B. Espion, Long-Term Sustained Loading Test on Reinforced Concrete Beams, Université Libre de Bruxelles Service Génie Civile, Brussels, 1988.

[5]   K.L. Scrivener, V.M. John, E.M. Gartner, Eco-efficient cements: Potential, economically viable solutions for a los-CO2, cement-based materials industry, Cem. Concr. Res. (2018) 1–25.

doi:10.1016/j.cemconres.2018.03.015.

[6]   Eurostat, Generation of waste by waste category, hazardousness and NACE Rev. 2 activity, Brussels, 2017.

[7]   R.V. Silva, J. De Brito, R.K. Dhir, Properties and composition of recycled aggregates from construction and demolition waste suitable for concrete production, Constr. Build. Mater. 65 (2014) 201–217. doi:10.1016/j.conbuildmat.2014.04.117.

[8]   N. Tošić, A. de la Fuente, S. Marinković, Creep of recycled aggregate concrete: Experimental database and creep prediction model according to the fib Model Code 2010, Constr. Build. Mater. 195 (2019) 590–599. doi:10.1016/j.conbuildmat.2018.11.048.

[9]   N. Tošić, S. Marinković, I. Ignjatović, A database on flexural and shear strength of reinforced recycled aggregate concrete beams and comparison to Eurocode 2 predictions, Constr. Build. Mater. 127 (2016) 932–944.

[10] J. Xiao, C.Q. Wang, J. Li, M. Tawana, Shake-table model tests on recycled aggregate concrete frame structure, ACI Struct. J. 109 (2012) 777–786.

[11] R.V. Silva, J. de Brito, R.K. Dhir, Establishing a relationship between the modulus of elasticity and compressive strength of recycled aggregate concrete, J. Clean. Prod. 112 (2016) 2171–2186. doi:10.1016/j.jclepro.2015.10.064.

[12] N. Tošić, A. de la Fuente, S. Marinković, Shrinkage of recycled aggregate concrete: experimental database and application of fib Model Code 2010, Mater. Struct. Constr. (2018). doi:10.1617/s11527-018-1258-0.

[13] N. Tošić, S. Marinković, J. de Brito, Deflection control for reinforced recycled aggregate concrete beams : Experimental database and extension of the fib Model Code 2010 model, Struct. Concr. (2019) 1–15. doi:10.1002/suco.201900035.

[14] R.V. Silva, J. de Brito, R.K. Dhir, Tensile strength behaviour of recycled aggregate concrete, Constr. Build. Mater. 83 (2015) 108–118. doi:10.1016/j.conbuildmat.2015.03.034.

[15] N. Tošić, S. Marinković, T. Dašić, M. Stanić, Multicriteria optimization of natural and recycled aggregate concrete for structural use, J. Clean. Prod. 87 (2015) 766–776.